University of Glasgow | Experimental Particle Physics

GLAS-PPE/2008-37
24th January 2008

Department of Physics and Astronomy
Experimental Particle Physics Group
Kelvin Building, University of Glasgow
Glasgow, G12 8QQ, Scotland
Telephone: +44 (0)141 330 2000 Fax: +44 (0)141 330 5881

Development of a high-speed single photon pixellated detector for visible wavelengths

Aaron Mac Raighne[1*], Antonio Teixeira[2], Serge Mathot[2], Jason McPhate[3], John Vallerga[3], Pierre Jarron[2], Colin Brownlee[4], Val O'Shea[1]

1. Department of Physics and Astronomy, University of Glasgow, Scotland.

2. CERN, Genève, Switzerland.

3. University of California, Berkeley, U.S.A.

4. The Marine Biological Association of the United Kingdom, Plymouth, England

Email: a.macraighne@physics.gla.ac.uk

Abstract

We present the development of a high-speed, single photon counting, Hybrid Photo Detector (HPD). The HPD consists of a vacuum tube, containing the detector assembly, sealed with a transparent optical input window. Photons incident on the photocathode eject a photoelectron into a large electric field which accelerates the incident electron onto a silicon detector. The silicon detector is bump bonded to a Medipix readout chip. This set-up allows for the detection and readout of low incident photon intensities at rates which are otherwise unattainable with current camera technology. Reported is the fabrication of the camera which brings together a range of sophisticated design and fabrication techniques and the expected theoretical imaging performace. Applications to cellular and molecular microscopy are also described in which single photon counting abilities at high frame rates are crucial.

* Corresponding author. Tel.: (+44) 141 330 4709; fax: (+44) 141 330 5299; e-mail: aaron.macraighne@gmail.com

1. Introduction

Biologists demand finer and finer resolution from their optical microscopy techniques as they strive to understand more complex cellular and molecular mechanisms. There are now many techniques in optical microscopy that reach, and in fact go beyond, the century old Abbe limit for optical microscopy resolution. Many of these techniques achieve higher contrast and higher resolution by collecting and imaging light from a very restricted area of the sample[1]. When this is considered with the fact that light yield from cellular fluorescence is inherently low,it results in the requirement of high gain, low light imaging detectors. This has led to the significant use of the Electron Multiplied CCD (EMCCD). The EMCCD is capable of fine resolution and low light imaging at high quantum efficiency but suffers from a low maximum frame rate ~500fps.

A very wide field of recent biological interest is in the imaging of Ca^{2+} signalling. An understanding of Ca^{2+} signalling is critical to the explanation of cellular biology. It lies at the fundamental level of inter-cell communication and intra-cellular process triggering. As such there are a number of different ion signalling entities that occur over different spatiotemporal domains which must be differentiated. An example of one such process is the imaging of calcium sparks, spatially-restricted fluctuations in the concentration of intra-cellular calcium, which occur over a 1-50ms time domain[2] with a minute variation in the fluorescence of the calcium-sensitive dye. The imaging and analysis of these and other rapid, localized cellular events requires a photon counting pixellated detector with sub millisecond resolution. It is applications such as these that have led to the design of the detector reported in this article.

2. The Medipix Chip

The Medipix read-out chip contains 256x256 pixels each with a square pixel size of side length 55 µm[3]. This chip is bump bonded to a 300µm thick silicon sensor[4]. Photons incident on the detector substrate create a charge cloud in the Si which is read at the input of the Medipix chip. The preamplifier has a gain ~13mV/1ke$^-$, a peaking time of 150ns and a return to baseline of <1µs, giving a count rate of 1MHz. A 13-bit counter per pixel is electronically shuttered when the chip is reading out. Using a clock of 100MHz and the parallel read-out the entire chip can be read-out in 266µs which makes possible the frame rates of over 3000fps. A full description of the chip, its operation and testing methods can be found in the thesis of Xavier Llopart[5]. Originally designed as a single photon counting device for x-ray imaging[6] we propose to exploit the advantages of the chip for the imaging of visible light.

3. Organisation Optical Imaging with Medipix, the electron bombarded Hybrid Photo Detector (HPD):

A HPD combines electron tube and semiconductor detector technology. The Medipix chip is mounted on a ceramic carrier (which will be described in further detail in the next section) and sealed within a vacuum tube. The end of the tube is covered by a transparent optical window onto which a photocathode has been deposited, Figure 1. An incident photon ejects a photoelectron from the photocathode. This electron is accelerated towards the silicon detector by the application of a high voltage across the tube, which defines the gain of the detector system. The electron can be accelerated to 5~10keV which results in a charge cloud in the detector much greater than the noise limit of the Medipix read-out chip.

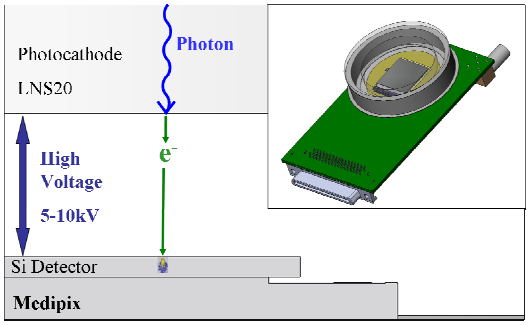

Figure 1. Schematic cross section illustration of the HPD internal structure. Subset is a schematic of the camera device connected to the read-out chipboard. The Medipix chip can be seen mounted on the Au ground of the multi-layer ceramic inside the vacuum tube.

If the charge deposited in the sensor is above the threshold value set on the Medipix, the internal counter in the pixel is incremented. The threshold is set at half the incident energy level of the incoming electrons in order to eliminate multiple hits in adjacent pixels[7].

4. Carrier Design and Fabrication

The Medipix chip is directly mounted on a ceramic header with a conductive epoxy. This carrier is a thick film multi chip module ceramic, which is fabricated by the sequential screen printing of gold trace layers and ceramic interstitial layers on a drilled ceramic header. The printing of each layer is done at room temperature, dried at 100°C and then fired for 10 minutes at 850°C, after which each layer is individually inspected for defects. The layout design is a modification of an earlier carrier designed by Vallerga *et al.*[8].

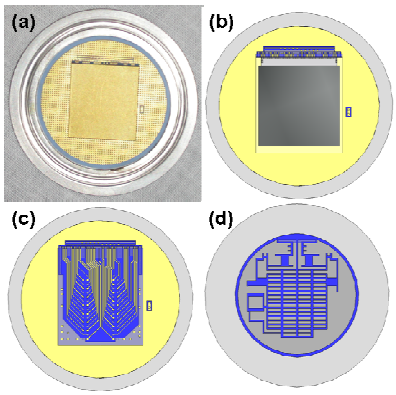

Figure 2. (a)Photograph of carrier with vacuum flange. (b) Schematic of the carrier and chip (c) Carrier with the mounting pad removed to show inner traces. (d) back of carrier showing pads for the connections of solderable parts.

Modification includes the introduction of a number of layers of offset gold pads and traces in ceramic to reduce the effect of micro-cracks in the gold, which can lead to leaks in the vacuum tightness of the carrier. It also included the redirection of all of the inner traces, the introduction of a greater number of vias to allow a lower resistance to ground and the inclusion of a high voltage trace to bias the Si detector. Figure 2(b) shows the design schematic of the carrier with the Medipix/detector assembly mounted. The wire traces within the layer and the component pads on the rear of the ceramic header can be seen in Figures 2 (c) and (d) respectively. A photograph of the ceramic in Figure 2(a) shows the ceramic and the Au pad on which the Medipix assembly will be mounted, also evident is the Kovar flange which is vacuum brazed to ceramic. The metal flange which surrounds the ceramic creates a base upon which the vacuum tube can be formed. The vacuum brazing of the Kovar flange and the alumina ceramic is made using two different brazing materials: Cusil-ABA and CB10 which are a Ag and Cu base alloy with Ti as an active element. The CB10 paste is laid down between the ceramic and the Kovar flange and the CuSil metallic wire is placed between the edge of the ceramic and the flange. These are heated in a vacuum oven with a controlled heating rate during which the brazing temperature is increased to a peak of 850 °C.

5. Imaging Performance

The Signal to Noise Ratio, Figure 3(a), was calculated according to the formulations put forward by Robbins[9], eqn. 1. The incoming photon flux is denoted by S, QE is the Quantum Efficiency, N is the read noise, M is the gain and D represents the dark noise. The read noise for the Medipix and the EMCCD is essentially zero; however an extra term, F, must be included for the electron multiplying step of the EMCCD.

$$SNR = S.QE \Big/ \sqrt{S.QE.F^2 + D.F^2 + \left(N/M\right)} \quad (1)$$

In this analysis F=1.4 for the EMCCD when working at high gain[9] and 1 for the Medipix. The SNR ratio of the Medipix HPD is lower than the EMCCD due to the low QE of the proposed photocathode (low-noise S20). By utilising a higher QE photocathode in future models we would expect the SNR of the HPD to outperform the EMCCD.

Figure 3(b) shows the calculated Modulation Transfer Function (MTF) for the HPD system. The MTF shown for the Medipix was calculated using the theory set-out by Passmore *et al.*[10]. This is then

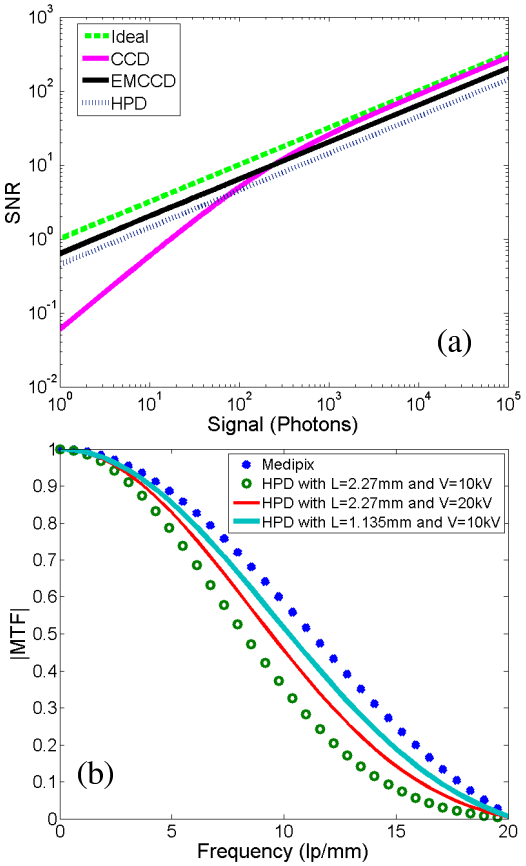

Figure 3: (a) Comparative theoretical SNR comparing the HPD to that of a typical CCD and EMCCD and the ideal, shot noise limited, detector. (b) MTF of the Medipix and of the Medipix HPD system, shown also are HPD systems with half the gap distance, L, and also double the gap voltage, V, to illustrate areas of possible improvement on the imaging performance.

multiplied by the theoretical MTF of the photocathode to find the MTF of the HPD system. The electron ejected from the photocathode will fall on the Medipix with a certain point spread function which is dependant on the material of the photocathode.The width of the point spread function is proportional to the gap distance between the photocathode and the detector substrate and inversely proportional to the square of the applied voltage across the gap[11]. The MTF of the system is limited by the Medipix and the effect of the photocathode can be minimised by increasing the voltage or decreasing the distance between the photocathode and the Medipix as is shown in Figure 3(b).

6. Conclusions

Many biological imaging applications require high frame rates at low light intensities. EMCCD cameras can achieve this but with frame rates limited to ~500fps. We present the design, and note the fabrication methods, of a detector capable of achieving unprecedented frame rates whilst maintaining SNR performance relative to the best EMCCD. MTF curves indicate expected contrast of 30% at spatial frequencies up to ~15 line pair/mm.

Acknowledgements:

The authors would like to thanks Thierry Gys, for his technical assistance on HPD design, Michael Campbell and Lukas Tlustos for their assistance on the Medipix and the bump bonding technology.

References

[1]D.J. Stephens, V.J. Allan, Science 300 (2003) 82.
[2]H.J. Knot, et al., Molecular Interventions 5 (2005) 112.
[3]L. Tlustos, R. Ballabriga, M. Campbell, E. Heijne, K. Kincade, X. Llopart, P. Stejskal, Ieee Transactions on Nuclear Science 53 (2006) 367.
[4]F. Quarati, V. O'Shea, K.M. Smith, Nuclear Instruments & Methods in Physics Research Section a-Accelerators Spectrometers Detectors and Associated Equipment 546 (2005) 42.
[5]X. Llopart Cudie, C. Frojdh, M. Campbell, Design and Characterization of 64K Pixels Chips Working in Single Photon Processing Mode, 2007.
[6]M. Campbell, E.H.M. Heijne, G. Meddeler, E. Pernigotti, W. Snoeys, Ieee Transactions on Nuclear Science 45 (1998) 751.
[7]G. McMullan, D.M. Cattermole, S. Chen, R. Henderson, X. Llopart, C. Summerfield, L. Tlustos, A.R. Faruqi, Ultramicroscopy 107 (2007) 401.
[8]J.V. Vallerga, J. McPhate, B. Mikulec, A. Tremsin, A. Clark, O. Siegmund, Noiseless imaging detector for adaptive optics with kHz frame rates, Advancements in Adaptive Optics, SPIE, Glasgow, Scotland, United Kingdom, 2004, pp. 1256.
[9]M.S. Robbins, B.J. Hadwen, Ieee Transactions on Electron Devices 50 (2003) 1227.
[10]M.S. Passmore, R. Bates, K. Mathieson, V. O'Shea, M. Rahman, P. Seller, K.M. Smith, Nuclear Instruments & Methods in Physics Research Section a-Accelerators Spectrometers Detectors and Associated Equipment 466 (2001) 202.
[11]I.P. Csorba, Applied Optics 16 (1977) 2647.